

Electrophysiological Activation and Propagation Times in the Ventricular Myocardial Band. First Study in Humans.

Activación electrofisiológica y tiempos de propagación en la banda muscular ventricular. Primer estudio mundial en seres humanos

JORGE C. TRAININI^{MTSAC, 1}, BENJAMÍN ELENCAWAJG², NÉSTOR LÓPEZ CABANILLAS^{MTSAC, 2}, JESÚS HERREROS³, NOEMÍ LAGO^{MTSAC, 4}, JORGE LOWENSTEIN^{MTSAC, 5}, ALEJANDRO TRAININI¹

I. FUNCTIONAL CONSIDERATIONS OF THE VENTRICULAR MYOCARDIAL BAND

After the analysis of the anatomical description of Torrent Guasp's ventricular myocardial band (1) (Figure 1) and the subsequent electrophysiological research that we performed in patients in previous studies, (2, 3) a clarifying interpretation of a few fundamental items is needed. Of the three spiral turns made by the descending segment in relation with the ascending segment, the first two successively pass at the front and behind the ascending segment, constituting the basal loop. (Figure 2). This last step, after the ventricular myocardial band folds and becomes the descending segment, is again behind the ascending segment; thus the helical disposition is lost in this spatial arrangement of the apical loop. This anatomical helical arrangement of the myocardial band segments keeps an important correlation with cardiac function. (4)

A ventricular narrowing movement occurs in the basal ventricular area of the heart. The phase of systolic narrowing (systolic contraction) starts with the consecutive activation of the right and left segments of the basal loop. The electrical activation progresses towards the descending band segment (axial activation) and simultaneously activates the ascending band segment (radial activation), as we have found in our investigations, (2, 3) (Figure 3) producing a helical torsion movement with subsequent shortening of the left ventricular vertical axis (ejection). The ventricular apex, constituted by the arrangement of the subepicardial fibers which become subendocardial with ventricular torsion, constitute a free apex with a pouch to bear intraventricular pressure exerted by the heart due to ventricular shortening. Then, the contraction of the ascending band segment, its stiffness and ven-

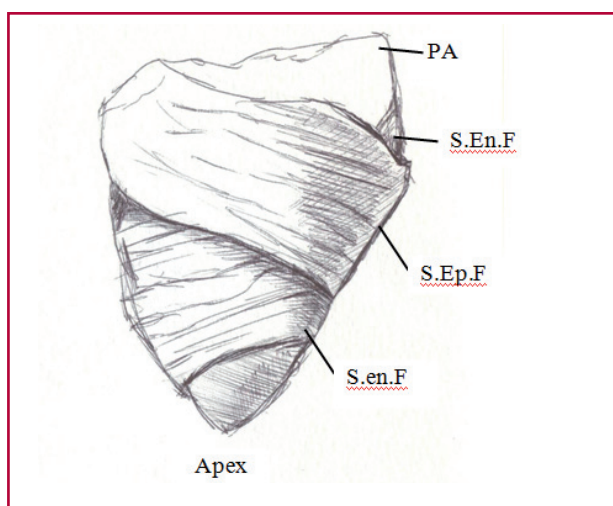


Fig 1. Right ventricular free wall. PA: pulmonary artery. S.En.F: Subendocardial fibers. S.Ep.F: Subepicardial fibers.

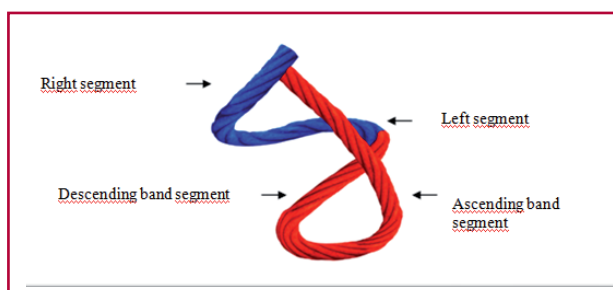


Fig 2. Ventricular myocardial band. The different segments of the ventricular myocardial band are shown. In blue: basal loop. In red: apical loop. Image in color available at the website.

REV ARGENT CARDIOL 2016;84:453-459. <http://dx.doi.org/10.7775/rac.v84.i5.9506>

Address for reprints: Dr. Jorge C. Trainini - Brandsen 1690 -3.er piso - Dpto. A - (1287) Ciudad Autónoma de Buenos Aires, República Argentina - e-mail: jctrainini@hotmail.com

^{MTSAC} Full Member of the Argentine Society of Cardiology

¹ Department of Cardiovascular Surgery, Hospital Presidente Perón. Buenos Aires, Argentina.

² Department of Electrophysiology, Hospital Presidente Perón. Buenos Aires, Argentina.

³ Chair of Cardiovascular and Thoracic Surgery. Universidad Católica San Antonio (UCAM). Murcia, Spain. Biomedical Engineering and Sanitary Technologies Foundation. Madrid, Spain.

⁴ Department of Cardiology, Hospital Presidente Perón. Buenos Aires, Argentina.

⁵ Department of Echocardiography, Investigaciones Médicas. Buenos Aires, Argentina.

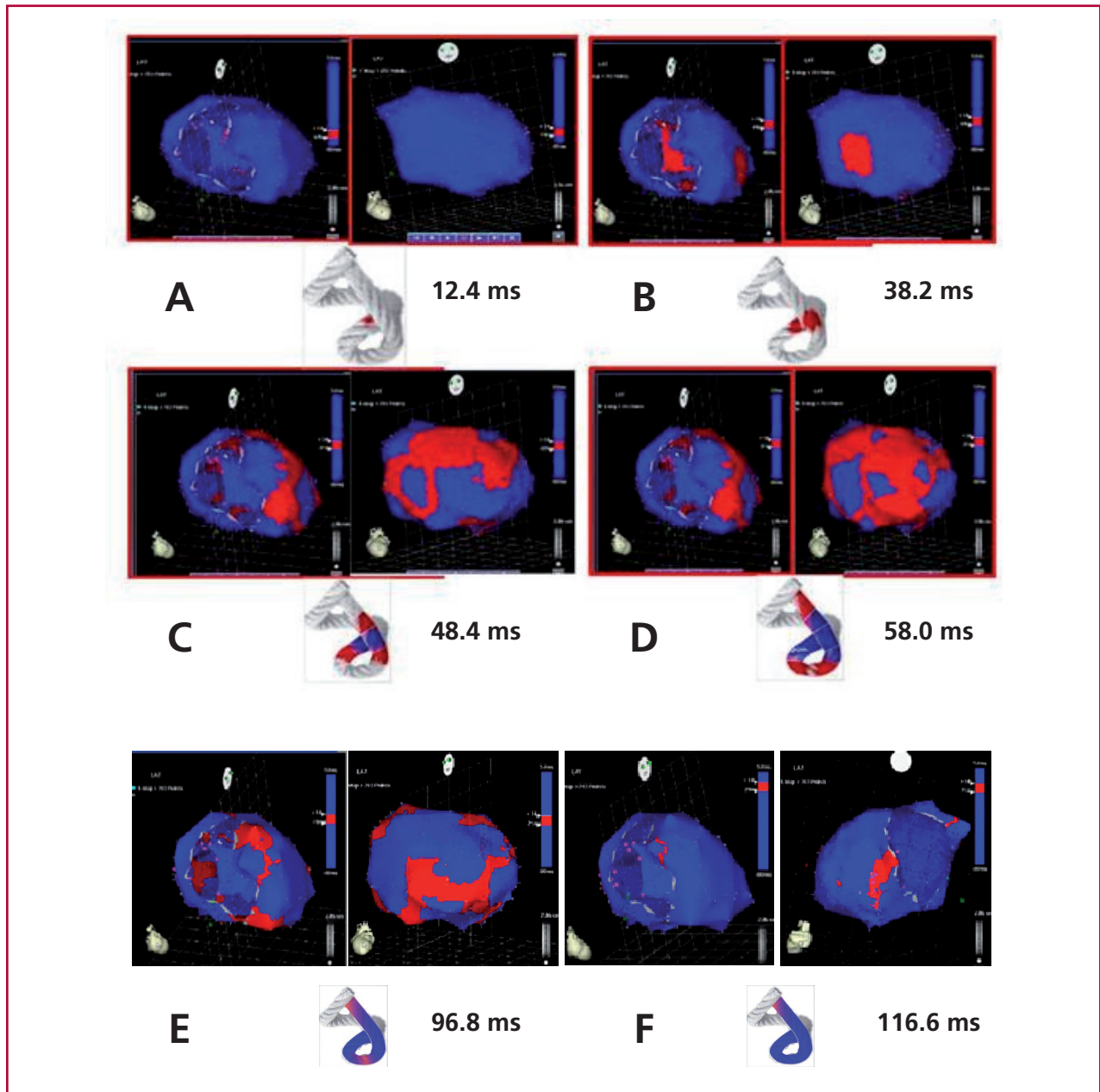


Fig. 3. A. Onset of left ventricular activation. The *left panel* shows the depolarization of the interventricular septum at 12.4 ms, corresponding to the descending band segment. In the *right panel*, the ventricular epicardium (ascending band segment) has not been activated yet. **B. Simultaneous activation of the band segments.** The activation progresses in the left ventricular septum through the descending band segment (axial activation) and simultaneously propagates towards the epicardium (radial activation) activating the ascending band segment at 38.2 ms. **C. Bidirectional activation of the apex and the ascending band segment.** The panel shows the end of septal activation, extending towards the apex, synchronously with the epicardial activation in the same direction. At the same time, the epicardial activation is directed towards the base of the left ventricle (48.4 ms). **D. Progression of activation.** The panel illustrates the progression of activation in the directions of the previous panel (58 ms). **E. Late activation of the ascending band segment.** At this moment, corresponding to approximately 60% of QRS duration, subendocardial activation (descending band segment) is already complete. The distal portion of the ascending band segment (epicardial segment) is depolarized later. This phenomenon correlates with its persistent contraction during the initial diastolic phase (988 ms). **F. Final activation.** The right panel shows the very late activation of the distal portion of the ascending band segment after 116.6 ms in a modified left anterior to left posterior-lateral oblique projection.

tricular lengthening determine an active mechanism during the isovolumic diastolic phase. This situation keeps the ventricle in an isovolumic state, but with a decrease of intraventricular pressure (untwisting and active suction) that is followed by atrioventricular valve the opening and ventricular filling (expan-

sion phase). Left ventricular shortening (descending movement of the ventricular base) and lengthening (ascending movement of the ventricular base) (5) correlate with Newton's law of action and reaction. (6)

As a consequence of the anatomic and functional process, under normal conditions, the annular nar-

rowing (a sphincter-like function) of the apex (the space between both band segments) is necessary to tolerate the retrograde pressure of the chamber produced by blood ejection.

During the initial isovolumic phase, which has been wrongly considered as part of diastole, but is an active process that should be referred to as suction phase, the persistent contraction of the ascending band segment with left ventricular lengthening causes a sufficient decrease of intraventricular pressure to produce ventricular suction. This fall in intraventricular pressure, found in our current investigations with cardiac resynchronization therapy, is produced due to persistent contraction of the ascending band segment during the isovolumic phase, and when the ventricle lengthens, it sucks blood by a suction mechanism similar to a “plunger” (suction phase). When this pressure is negative enough (<10 mm Hg) and the ventricle has lengthened and “untwisted”, the mitral valve opens and the ventricle is abruptly filled with blood coming from the atrium (filling phase). (7-10)

The circulatory system of annelids uses a peristaltic movement for the progression of contraction. Propagation of contraction follows the pattern of axial activation, but after the evolutionary twisting of the circulatory system in birds and mammals, radial activation develops (Figure 3B). In this way, both band segments present the helical movement necessary to produce the associated movements of ventricular torsion and untwisting-suction.

The helical ventricular myocardial band of *Torrey-Guasp* has been criticized because it is difficult to visualize. On the contrary, the images obtained with magnetic resonance imaging (11, 12) and the logical evolutionary phylogenetic concept is against these criticisms. Born as a loop of the arterial semicircle of amphibians and reptiles as adaptation to terrestrial life, the myocardial fibers intensely joined in their contact surfaces, constituting the myocardial band segments. Birds and mammals required this fiber arrangement to eject blood flow into two circulatory systems (systemic and pulmonary circulation) at a high velocity and in a short period of time. The mechanical efficiency obtained by the mechanisms of ventricular torsion and untwisting could not be modified, as, since the beginning of the evolutionary process, these mechanisms depended on the propagation of the electrical impulse through the anatomical pathways. (13, 14)

The fact that the descending band segment makes two turns behind the ascending band segment without entwining is explained by ontogeny. Thus, a distal cardiac zone (apex) is created that contains the residual systolic blood volume, where the helical movement has lower amplitude, with a first turn to the left during systole (seen from the apex) and then to the right at the beginning of the suction phase, with the contraction of the ascending band segment. Also, the api-

cal loop has an accordion-like movement that shortens in systole and lengthens during the isovolumic phase (active suction). This longitudinal movement of apex-base contraction during systole and lengthening during the isovolumic phase accounts for 75% of the left ventricular capability of ejection and suction, respectively. The transverse interaction of narrowing (in systole) and widening (in diastole) of the basal loop contributes with only 25% of ventricular volume.

As the maximal reduction in ventricular pressure is achieved in only 15-20% of diastole, it is reasonable to think that diastole is an active mechanical process and not just simple passive relaxation. The time taken by diastole to achieve its maximal negative pressure (120 ms) is similar to the time taken by systole to achieve its highest ejective pressure (140 ms). The architecture of the sarcomere in the spatial integration and its contractile scaffolding and biochemical conformation, implies the presence of elastic properties added to the active phase. The activation of the ascending band segment generates a negative intraventricular pressure by acting on the elastic myocardial properties in order to attain the optimal elastic recoil of the sarcomeres in terms of adequate time and relaxation. Breaking this limit in elastic recoil imposed by the muscle architecture of the heart will impact on the development of heart failure. (15)

Residual systolic blood volume represents 30% of the total end-diastolic volume. Between systole and diastole, the left ventricle is a closed chamber filled up with incompressible blood so that its volume cannot change regardless of the degree of muscle contraction. Therefore, this phase is isovolumic, and as muscle contraction cannot modify the blood volume, intraventricular pressure decreases, favoring diastolic filling. Under these conditions, the reduction of intraventricular pressure will depend on the ability of muscle contraction and the geometry of the chamber affecting the distribution of pressures. The presence of an incompressible fluid and the geometry of the chamber containing blood volume are necessary, from the point of view of physics, to produce a significant reduction of intraventricular pressure favoring a “plunger effect”.

There is a range of residual systolic blood volume that is optimal for suction. If blood volume is higher, muscle contraction must increase to create the necessary fall in pressure. On the contrary, if blood volume is lower, the interaction between the walls will hinder the suction mechanism and the boundary layer phenomena in diastole will alter ventricular filling. From a physical point of view, an increased end-systolic volume will affect the suction mechanism which will be thus related with the volume ejected during systole.

II. PROPAGATION TIMES OF ELECTRICAL ACTIVATION THROUGH THE VENTRICULAR MYOCARDIAL BAND

The sequence of left ventricular endocardial and epicardial electrical activation was studied in five adult

patients aged between 19 and 42 years using three-dimensional electroanatomic mapping with the Carto navigation and mapping system (Biosense Webster, California, USA), which allows a three-dimensional anatomical representation with activation maps and electrical propagation. The propagation time of electrical activation was measured in milliseconds (ms). Isochronic and activation sequence maps were constructed and correlated with the surface electrocardiogram. Apical, lateral and basal views were obtained. As the myocardial structure has an endocardial portion and an epicardial portion, called by Torres Guasp descending band and ascending band, respectively, (1) two sites of puncture were used for mapping. (16)

Figure 3 shows the propagation of endocardial and epicardial activation. In every pair of figures, the left panel shows the right lateral projection and the right panel shows the simultaneous left anterior oblique projection. The activated zones at each moment are shown in red. The activation of the descending band and ascending band segments constituting the left ventricular muscle structure in the rope model is rep-

resented below each pair of figures. (1) The depolarized area at that moment is represented in red and those areas previously activated and in refractory period are represented in blue. Mean propagation time of the electrical activation through the ventricular myocardial band (in ms) is observed beside each rope (see also Tables 1 and 2).

The activation of the left ventricle initiates in the interventricular septum, 12.4 ± 1.816 ms after activation starts (Figure 3A). An epicardial area is also activated at that moment -the ascending band segment- evidencing radial activation at a point that we called the “crossing of band segments”. This activation starts 25.8 ± 1.483 ms after septal stimulation (Figure 3B, Table 2) and 38.2 ± 2.135 ms after the initiation of cardiac activation. Simultaneously, it extends axially towards the ventricular apex, following the anatomical arrangement of the descending band segment at a mean time of 58 ± 2.0 ms (Figure 3C and D, Table 1). After the “crossing of band segments”, the activation loses its unidirectional character and becomes more complex. Three simultaneous wave-

	Case 1	Case 2	Case 3	Case 4	Case 5	Mean	SD
Figure 3 A	10	12	13	15	12	12.4	1.816
Figure 3 B	35	38	37	41	40	38.2	2.135
Figure 3 C	45	47	49	52	49	48.4	2.332
Figure 3 D	55	59	57	61	58	58.0	2.000
Figure 3 E	94	98	98	99	95	96.8	1.939
Figure 3 F	115	118	114	120	116	116.6	2.154

SD: Standard deviation.

Table 1. Activation times (in milliseconds)

Case 1	Case 2	Case 3	Case 4	Case 5	Mean	SD
25	26	24	26	28	25.8	1.48

SD: Standard deviation.

Table 2. Time of radial propagation (from the descending band segment to the ascending band segment) (in milliseconds)

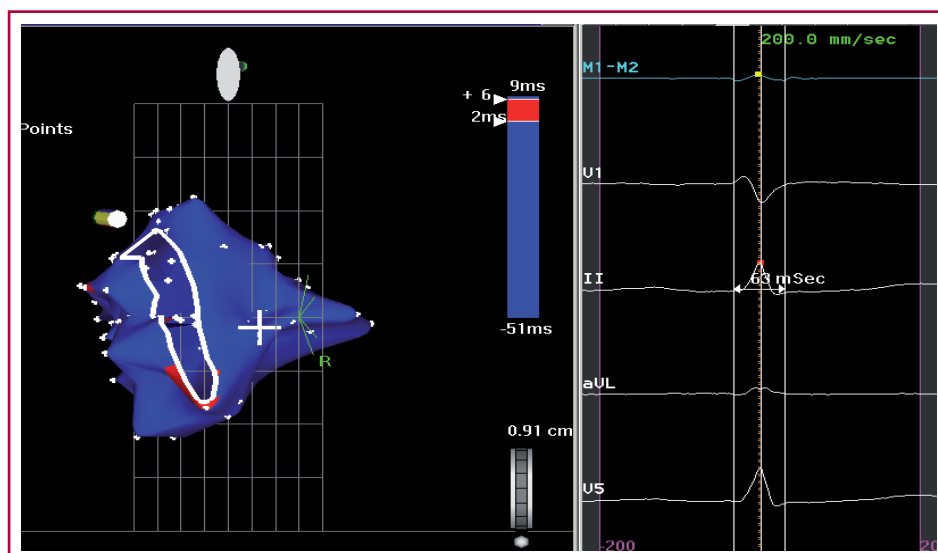


Fig. 4. Endocardial activation ends in the area corresponding to the mitral annulus. Overall endocardial activation “occupies” approximately 60% of QRS duration (line D in the right panel). Epicardial activation probably started before, but surely it ends during the final part of the QRS.

fronts are generated: 1) the distal activation of the descending band segment towards the apical loop; 2) the depolarization of the ascending band segment from the crossing point towards the apex; and 3) the activation of this band segment from the crossing point towards the final end of the muscular band in the aorta. Figures 3 D, E and F show the progression and end of this process. The endocardial activation finishes well before the end of the QRS (Figure 4); the rest of this process corresponds to late activation of the distal portion of the ascending band segment, which explains its persistent contraction during the isovolumic diastolic phase, basis of the mechanism of ventricular suction (Figure 3F).

III. ECHOCARDIOGRAPHIC CONCEPTS

Currently, echocardiography is capable of providing non-invasive information about the complex mechanism of myocardial contraction. The analysis of 2D myocardial strain based on speckle tracking echocardiography demonstrates opposing rotation of the left ventricular apex and base, which produces ventricular torsion (systolic contraction) and subsequent untwisting (suction mechanism, “plunger effect”) (Figure 5). As seen from the apex, counterclockwise rotation (apical rotation) is expressed as a positive value and clockwise rotation (basal rotation) is expressed as a negative one. Left ventricular torsion is calculated as the difference between the counterclockwise apical rotation curve (positive) and clockwise basal rotation curve (negative). In normal subjects, this value is about $+11^\circ$, and apical rotation predominates.

Deviation of this value is generally a marker of heart disease; yet, it should be noted that the normal values of left ventricular rotation and torsion can vary and depend on the technique used, the location of the area or interest (subendocardium or subepicardium), age and loading conditions. (17)

The radius of subepicardial rotation is greater

than that of the subendocardium. The subepicardium consequently provides greater torque than the subendocardium, and as a result subepicardial rotation is more significantly expressed at the apical level.

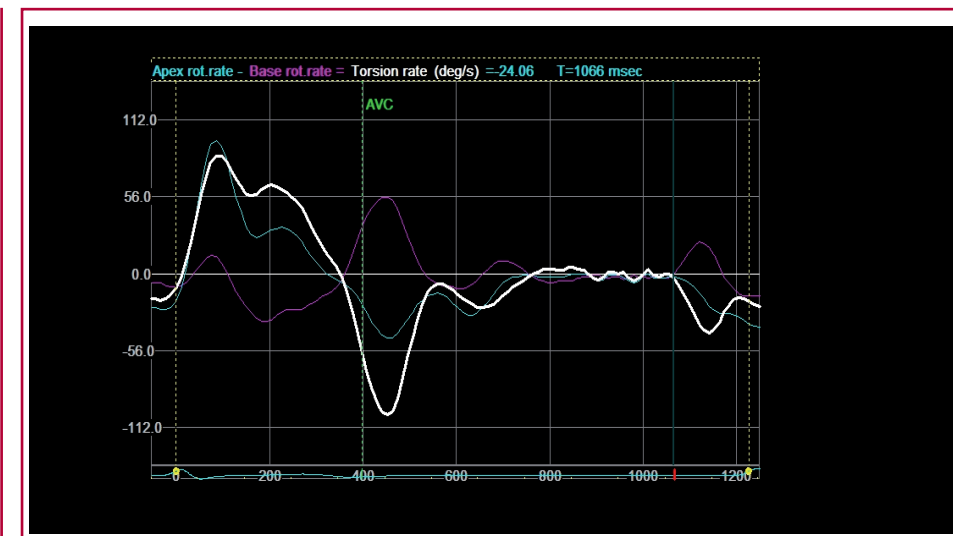
In dilated cardiomyopathy, impairment of left ventricular systolic torsion is proportional to the level of left ventricular dysfunction and is related with reduced amplitude of rotation at the apex, while basal rotation can be normal or reduced. In some of these patients, the apex and the base rotate in the same clockwise direction. A rapid normalization in patients responding to cardiac resynchronization therapy can predict inverse remodeling at 6 months.

In summary, the novel echocardiographic techniques support the morphological distribution of the “ventricular myocardial band” and provide additional information about the significant impairment imposed by a deficit in atrioventricular synchrony which significantly improves with resynchronization therapy.

IV. INTRAVENTRICULAR PRESSURE AND SUCTION MECHANISM

During cardiac resynchronization therapy, we measured intraventricular pressure to achieve evidence of improved suction mechanism in the isovolumic diastolic phase. Figure 6 A shows the left ventricular pressure curve in a patient with left bundle branch block before implanting a cardiac resynchronization therapy device. The hypothesis is that left bundle branch block modifies left ventricular activation sequence and, in consequence, mechanical sequence is also impaired. Thus, the sequential activation of the band segments is also impaired and the suction mechanism is lost. Consequently, diastolic pressure increases. Stimulation of the left ventricular endocardium (the area corresponding to crossing of band segments) in cardiac resynchronization therapy would reestablish the normal electrical activation and mechanical sequence of

Fig. 5. Peak torsion and untwisting velocities.



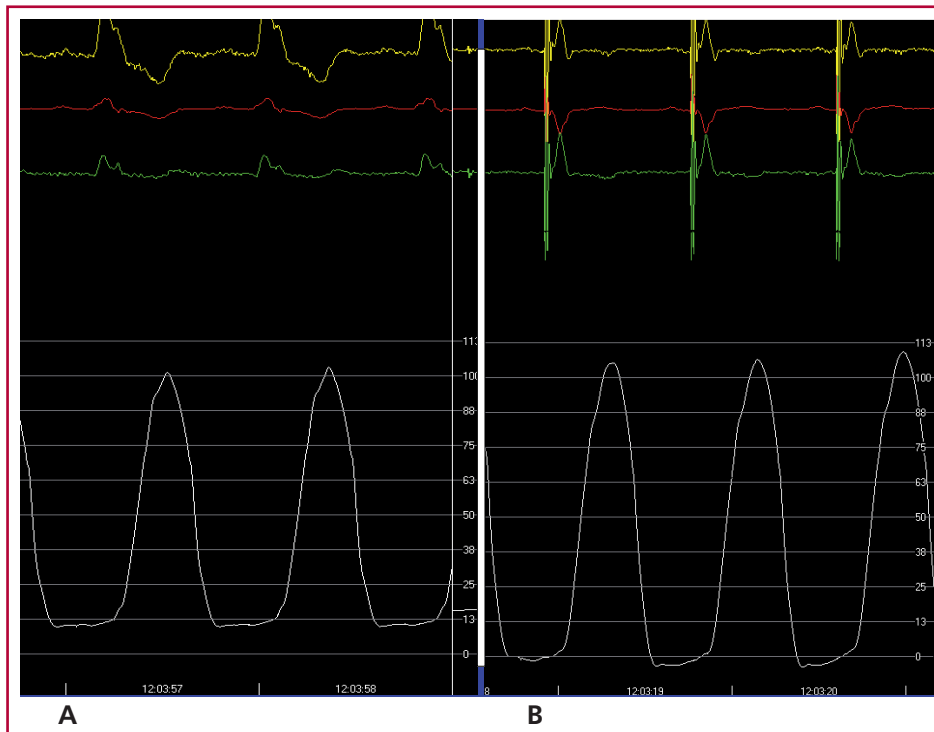


Fig. 6. Left ventricular pressure curve in a patient before (A) and after (B) cardiac resynchronization therapy.

both band segments. The suction mechanism would also be restored and left ventricular diastolic pressure would decrease (Figure 6 B), improving heart failure symptoms.

V. THE JURDHAM PROCEDURE

The Jurdham procedure consists in inserting an endocardial left ventricular lead from the right atrium via a femoral transeptal sheath for cardiac resynchronization therapy. (18,19) A right femoral approach is used and the lead is then tunneled to the subclavian vein. The technique has been proved to be feasible and safe without significant complications, but lacked a physiological explanation of its benefits. At the same time, our team was capable of evaluating the normal sequence of left ventricular endocardial and epicardial electrical activation using three-dimensional electroanatomic mapping with the Carto navigation and mapping system, confirming physiological effects as systolic ventricular torsion and the effect of active suction in the isovolumic diastolic phase.

From the perspective of our investigations, the explanation becomes much more coherent in the effect achieved with this resynchronization technique. Cardiac resynchronization therapy via the endocardial approach would restore normal electrical activation in the ventricular myocardial band and, consequently, in mechanical function.

Conflicts of interest

None declared. (See authors' conflicts of interest forms in the website/Supplementary material).

REFERENCES

1. Torrent Guasp F. Estructura y mecánica del corazón. Barcelona: Grass Ed; 1987.
2. Trainini JC, Elenchwajg B, López-Cabanillas N, Herreros J, Lago N, Lowenstein JA et al. Fundamentos de la nueva mecánica cardíaca. La bomba de succión. Buenos Aires: Ed Lumen; 2015.
3. Trainini JC, Elenchwajg B, López-Cabanillas N, Herreros J, Lago N, Lowenstein JA. Electrical Propagation in the Mechanisms of Torsion and Suction in a Three-phase Heart. *Rev Argent Cardiol* 2015;83:420-8. <http://doi.org/bqqc>
4. Carreras F, Ballester M, Pujadas S, Leta R, Pons-Lladó G. Morphological and functional evidences of the helical heart from non-invasive cardiac imaging. *Eur J Cardiothorac Surg* 2006;29(Suppl 1):S50-5. <http://doi.org/cmj4sn>
5. Sengupta PP, Khandheria BK, Kornek J, Wang J, Jahangir A, Seward JB, et al. Apex-to-base dispersion in regional timing of left ventricular shortening and lengthening. *J Am Coll Cardiol* 2006;47:163-72. <http://doi.org/c79bb9>
6. Trainini JC, Herreros J, Cabo J, Otero Coto E, Cosín Aguilar J. The cardiac pump section. The application of the myocardial band of Torrent-Guasp to the surgical treatment of heart failure. *Cir Cardiovasc* 2011;18:103-12. <http://doi.org/f2j8ts>
7. Cosín Aguilar J, Hernández Martínez A, Tuzón Segarra MT, Agüero Ramón-Llin J, Torrent Guasp F. Estudio experimental de la llamada fase de relajación isovolumétrica del ventrículo izquierdo. *Rev Esp Cardiol* 2009;62:392-9. <http://doi.org/ccnmdc>
8. Buckberg GD, Coghlan HC, Torrent Guasp F. The structure and function of the helical heart and its buttress wrapping. V. Anatomic and physiologic considerations in the healthy and failing heart. *Semin Thorac Cardiovasc Surg* 2001;132:358-85. <http://doi.org/6tk>
9. Torrent Guasp F, Buckberg G, Carmine C, Cox J, Coghlan H, Gharib M. The structure and function of the helical heart and its buttress wrapping. I. The normal macroscopic structure of the heart. *Semin Thorac Cardiovasc Surg* 2001;13:301-19. <http://doi.org/6tk>
10. Trainini JC, Andreu E. ¿Tiene significado clínico la remodelación reversa quirúrgica del ventrículo izquierdo? *Rev Argent Cardiol* 2005;73:44-51.
11. Poveda F, Gil D, Martí E, Andaluz A, Ballester M, Carreras F. He-

- lical Structure of the Cardiac Ventricular Anatomy Assessed by Diffusion Tensor Magnetic Resonance Imaging With Multiresolution Tractography. *Rev Esp Cardiol* 2013;66:782-90. <http://doi.org/f2fnsh>
12. Wu MT, Tseng WYI, Su MYM, Liu ChP, Chiou KR, Wedeen VJ, et al. Diffusion tensor magnetic resonance imaging mapping the fiber architecture remodeling in human myocardium after infarction. Correlation with viability and wall motion. *Circulation* 2006;114:1036-45. <http://doi.org/djq4t5>
13. Torrent Guasp F. La estructuración macroscópica del miocardio ventricular. *Rev Esp Cardiol* 1980;33:265-87.
14. Torrent Guasp F. Estructura y función del corazón. *Rev Esp Cardiol* 1998;51:91-102. <http://doi.org/6tj>
15. Cosín-Aguilar J, Hernández Martínez A. The Band Arrangement of Myocardial Fibres Determines Cardiac Morphology and Function. *Rev Esp Cardiol* 2013;66:768-70. <http://doi.org/f2fnsp>
16. Sosa E, Scanavacca M, d'Avila A, Pilleggi F. A new technique to perform epicardial mapping in the electrophysiology laboratory. *J Cardiovasc Electrophysiol* 1996;7:531-6. <http://doi.org/dzc5pw>
17. Cheng A, Nguyen TC, Malinowski M, Daughters GT, Millar DC, Ingels NB Jr. Heterogeneity of left ventricular wall thickening mechanisms. *Circulation* 2008;118:713-21. <http://doi.org/cxfhz3>
18. Elencwajg B, López-Cabanillas N, Cardinali E, Trainini JC. Ventricular Resynchronization: A New Technique and Device for Endocardial Left Ventricular Lead Placement. *Rev Argent Cardiol* 2010;78:143-6.
19. Elencwajg B, López-Cabanillas N, Cardinali EL, Barisani JL, Trainini J, Fischer A, et al. The Jurdham procedure: endocardial left ventricular lead insertion via a femoral transseptal sheath for cardiac resynchronization therapy pectoral device implantation. *Heart Rhythm* 2012;9:1798-804. <http://doi.org/bqqd>